RESEARCH PAPER

Synthesis and electrochemical properties of different sizes of the CuO particles

**Xiaojun Zhang · Dongen Zhang · Xiaomin Ni ·
Jimei Song · Huagui Zheng**

Abstract Well-dispersed cupric oxide (CuO) nanoparticles with the size from 10 to 100 nm were successfully synthesized by thermal decomposition of CuC_2O_4 precursor at 400 °C. The prepared CuO nanoparticles of different sizes used as anode materials for Li ion battery all exhibit high electrochemical capacity at the first discharge. However, with the particles size changing, an interesting phenomenon appears. That is, the larger size of the particles is, the discharge capacity of the first time smaller is, while that of the second time is larger. At the same time, the mechanism of the above phenomenon is discussed in this paper. Surprisingly, we have synthesized the copper nanoparticles with different sizes by the CuO of different sizes as the electrodes.

Keywords Electronic materials ·
Oxides · Inorganic compounds · Chemical synthesis ·
Electrochemical properties · Thermal decomposition

Introduction

Since the early 1990s, people everywhere have been enjoying the great convenience brought about in daily life through the use of rechargeable lithium-ion batteries (LIBs) (Ozawa 1994). Compared with other battery systems, LIBs show the advantages of high energy density, long cycle and shelf life, and no memory effect. The search for better electrode materials has been the most dynamic motivation behind the research and development of LIBs (Scrosati 1995; Wang et al. 2005; Ritchie and Howard 2006; Liu et al. 2006; Ng et al. 2006). The most attractive research in this respect directed towards both improving the state-of-the-art electrode materials, i.e. $LiCoO_2$, $LiNiO_2$ and $LiMn_2O_4$ for the positive electrode, and exploring alternative electrode materials with superior properties (Kalaiselvi et al. 2003; Zhang et al. 2006; Zhou et al. 2005a, b; Ha et al. 2006; Kim et al. 2006). As the negative electrode, some metal oxides such as ZnO, NiO, MnO_2, SnO_2 and CuO are promising candidates (Zhou et al. 2005a, b; Wang et al. 2005; Park and Yoon 2003; Yuan et al. 2006). Among those metal oxides, copper oxide (CuO), as a p-type semiconductor has been found widespread application in many areas such as high temperature superconductors, optical switching and anode materials (Poizot et al. 2000; Tarascon and Armand 2001; Grugeon et al. 2001; Shembel et al. 2005). For rechargeable batteries, copper oxide electrode has been found to have high capacity density and good capacity retention for lithium insertion and extraction (Chang et al. 2003; Gao et al. 2004). As CuO is a new electrode material with good electrochemical performance, study of the mechanism of the reaction of CuO electrode with Li is

X. Zhang · D. Zhang · X. Ni · J. Song · H. Zheng (✉)
Department of Chemistry, University of Science
and Technology of China, Hefei, Anhui 230026,
People's Republic of China
e-mail: zhangxiaojun@ustc.edu

also one of the most active areas (Zhang et al. 2004, 2005; Grugeon et al. 2001).

In this work, well-dispersed CuO nanoparticles with the size from 10 to 100 nm were successfully synthesized by a facile way. With the particles size changing, an interesting phenomenon appears. That is, the size of the particles is larger, the discharge capacity of the first time is smaller, while that of the second time is larger. We have discussed the mechanism of the above appearance. At the same time, we have synthesized the copper nanoparticles with different sizes by used the cupric oxide with different sizes as the electrodes.

Experimental

In a typical process, analytic grade $Cu(NO_3)_2$ was dissolved in 40 mL distilled water to form a transparent solution. Then oxalic acid dissolved in an equal volume of distilled water was dropwise added to the above solution under magnetic stirring. After stirring for about 2 min, the suspension colloids were washed with distilled water and ethanol for several times to purify the product. Then the product was dried at 50 °C for 12 h. Finally the obtained copper oxalate precursor was heated to 400 °C at a ramping rate of 10 °C min^{-1} and calcined at 400 °C for 4 h.

The samples were characterized by means of their X-ray powder diffraction (XRD) patterns with a Philips X'Pert Super diffractometer with graphite monochromatized Cu Kα radiation ($\lambda = 1.54178$ Å) in the 2θ range of 10–80̊. The field emission scanning electron microscopy (FE-SEM) images were taken using a JEOL JSM-67700F SEM.

The electrochemical tests were conducted with a Teflon cell. The working electrode was a mixture of CuO nanoparticles/acetylene black/polyvinylidene fluoride (PVDF) with weight ratio 80/10/10. Metallic lithium was used as the reference electrode. The cells were assembled in a glove box filled with highly pure argon gas (O_2 and H_2O levels <5 ppm). The cell was galvanostatically cycled in the 3.5–0.5 V range at a current density of 0.1 mA cm^{-2}.

Results and discussion

As shown in Table 1, with the amount of $Cu(NO_3)_2$ decreasing, the size of the obtained CuO particles

Table 1 Different molar rate of the $Cu(NO_3)_2$ (mmol) and $H_2C_2O_4$ (mmol) due to the different crystalline size (nm)

Number	$Cu(NO_3)_2$	$H_2C_2O_4$	Size
1.	10	5	10
2.	8	5	20
3.	6	5	40
4.	4	5	70
5.	2	5	100
6.	10	4	10
7.	10	2	10
8.	10	1	10

increased. In order to investigate the effect of the ratio on the size of the CuO particles, we changed the amount of the $H_2C_2O_4$ in the reaction and kept the other conditions as the same, the size of the CuO particles nearly did not change. In order to discuss the negative ion effect, we used $CuCl_2$ or $CuSO_4$ instead of $Cu(NO_3)_2$, the size of the particles is almost the same as that of the method with $Cu(NO_3)_2$. So we supposed the size of the particles may be attributed to the effect of the concentration of Cu^{2+}.

In order to investigate the mechanism more easily and conveniently, we took sample 1, 3, and 5 as our study object in the following discussion.

XRD analysis is used to determine the structure and phase of the sample 1, 3, and 5. Figure 1 shows the XRD patterns of the samples. All the peaks can be clearly indexed to monoclinic-phase CuO (space group C2/c). Compared with the standard diffraction
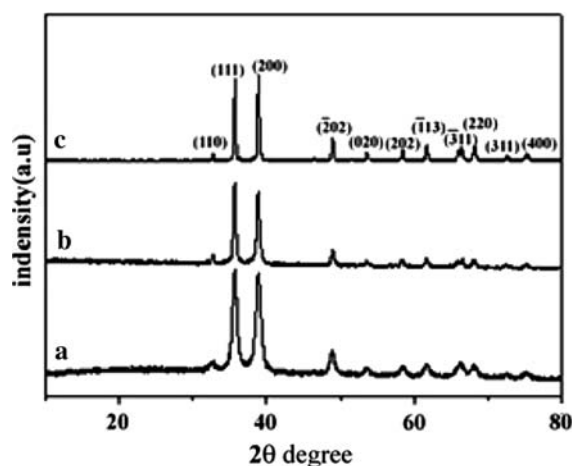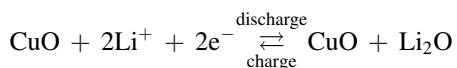

Fig. 1 XRD patterns of the as-prepared CuO nanoparticles (**a**) sample 1, (**b**) sample 3, (**c**) sample 5

peaks (JCPDS Card No. 41–0254), no other peak is observed belonging to the impurities, such as CuC_2O_4 or Cu_2O, indicating the high purity of as-obtained samples. According to the Debye–Scherrer equation, the average crystalline diameter of the obtained CuO particles is about 10 nm (a), 40 nm (b), 100 nm (c) of sample 1, 3, and 5, respectively.

The morphology of the product is examined by FESEM. From the FESEM image of nanostructures CuO (Fig. 2), the average particle size is about 10, 40 and 100 nm with narrow size distribution, according with the calculated value. The HRTEM image (Fig. 3) exhibits that regular spacing of the clear lattice planes is ~ 0.274 nm, which correspond well to (-110) planes of monoclinic-phase CuO.

Figure 4 shows the potential-capacity curves for the CuO/Li cell at a current density of 0.1 mA cm^{-2}. When Li is inserted into CuO in the first discharge, there are two obvious sloping potential ranges (1.2–0.8 and 0.8–0 V versus Li$^+$/Li) for the lithium reaction with the CuO nanoparticles, corresponding to Li insertion into the crystal lattice of CuO (Novak 1985; Novak et al. 1985; Podhajecky 1985). As

shown in the Fig. 4 of a, b, c, a common appearance of them existed. That is, there is an additional plateau at 2 V in the first discharge curve after close observation. It may be attributed to the reduction of O_2 and H_2O (Podhajecky et al. 1985). So the participation of O_2 and H_2O cannot be excluded, since these species are known to be strongly absorbed on the CuO surface. After the first charge, the plateau disappears because O_2 and H_2O absorbed on the CuO surface decrease completely. Therefore, in the following discharge curves, there exists no substantial change in the curve shape. And from the Fig. 4, we know that the initial discharge capacity of the sample 1, 3, 5 is 810, 795, 776 mA h g^{-1}, which corresponds to a consumption of 2.47, 2.37, 2.32 Li per CuO, respectively, larger than the value calculated from the stoichiometric formula demands. The overall electro-chemical process can be expressed as follows:

$$CuO + 2Li^+ + 2e^- \underset{charge}{\overset{discharge}{\rightleftarrows}} CuO + Li_2O$$

After the comparison of the data from both the first discharge and the second discharge of all the particles

Fig. 2 SEM images of the as-prepared CuO nanoparticles (**a**) sample 1, (**b**) sample 3, (**c**) sample 5
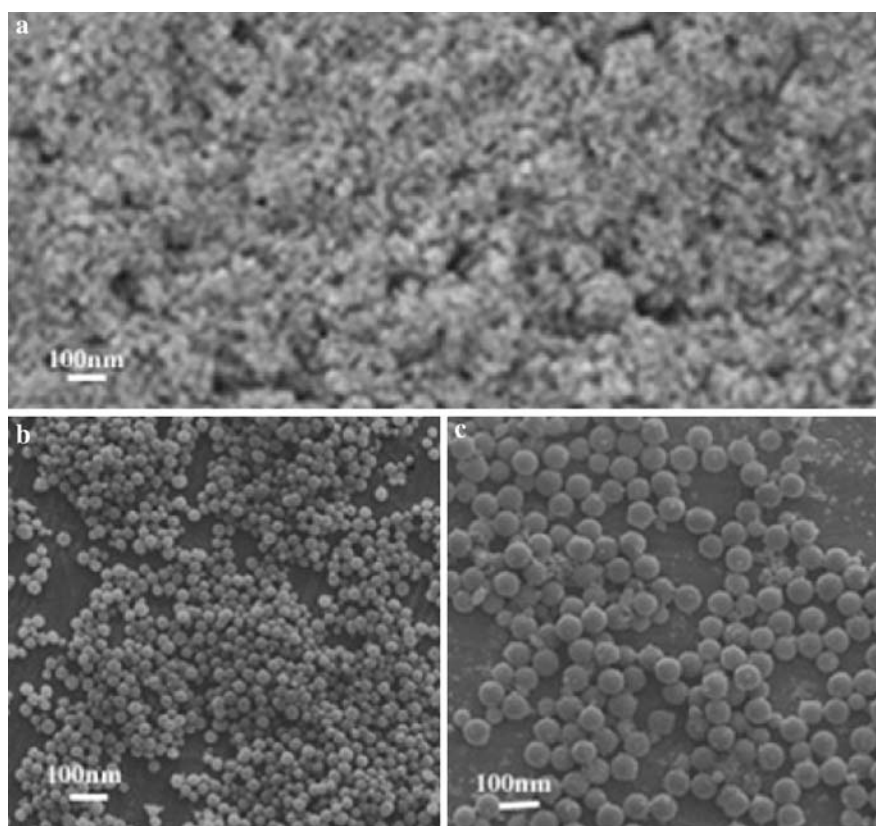
Fig. 3 (**a**) High-
magnification HRTEM
image of the sample1, (**b**)
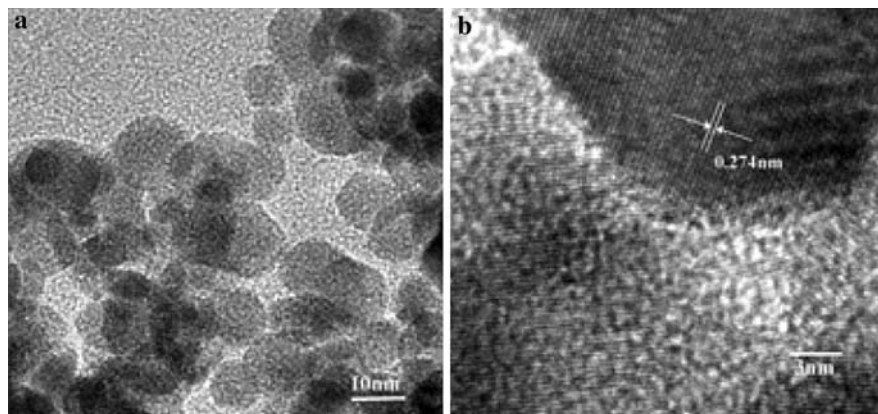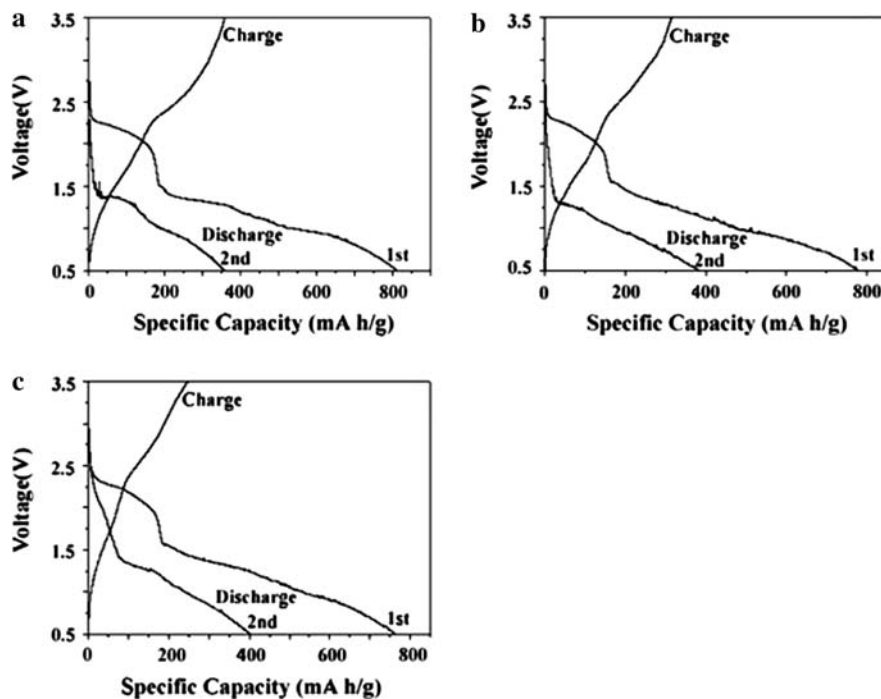corresponding HRTEM
image of this nanoparticle

Fig. 4 First and second
discharge of the different
average diameter of the as-
prepared CuO nanoparticles
(**a**) sample 1, (**b**) sample 3,
(**c**) sample 5

of the three different sizes (Fig. 4 a, b, c), an interesting rule was found. With the particles size increasing, the first discharge capacity decreased while the second discharge capacity increased. We think if the CuO particles size is larger, the smaller specific surface area of CuO may lead to the decrease of the capacity of the first discharge. So the first discharge capacity decreased. At the same time according to Tarascon's studies (Grugeon et al. 2001; Debart et al. 2001), the electrochemical reduction process of CuO includes a phase transition into Cu_2O and the subsequent formation of Cu nanoparticles,

and then a part of Cu nanoparticles will be coated by the organic-type. And if the size of the Cu particles is larger, they are more difficult to be coated by the organic-type and to dissolve into the electrolyte. In our experiment we suggest that the larger size CuO particles is, the larger Cu particles form (proved in our following discussion). Therefore, the large size CuO particles will induce more Cu particles take part in the next step of the cell reaction after the first discharge, which may results in the increase of the capacity of the second discharge.
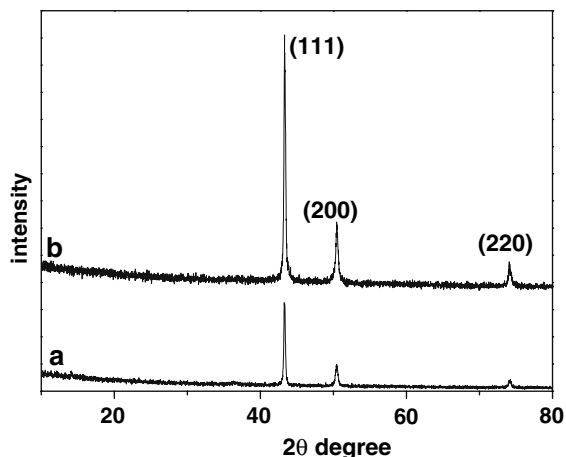
Fig. 5 The XRD patterns of Cu particles by treated at the first discharged electrode (**a**) electrode a, (**b**) electrode c

In order to prove the above suggestion, the CuO electrode (a and c) after the first discharge was treated with NMP (N-Methyl−2-Pyrrolidone) and hydrochloric acid. Pure metallic copper powder with face-centered cubic crystal structures was obtained as shown in the XRD pattern of the isolated copper particles (Fig. 5). The rather sharp diffraction peaks suggest a high crystalline of these copper particles with an average crystallite size of 10 nm (Fig. 5a) and 100 nm (Fig. 5b), which is calculated with the Scherrer equation. The FESEM image of the copper particles (Fig. 6) reveals that the final solid product consists of a large quantity of uniform nanoparticles with a particle size of about 10 nm (Fig. 6a) and a less quantity of uniform nanoparticles with a particle size of about 100 nm (Fig. 6b), respectively.

According to the analysis of the XRD and FESEM of the as-prepared products after the first discharge, we think that after the first discharge almost all of the CuO particles changed to the Cu particles. And the size of the particles did not change before and after the discharge. Hence, we think this electrochemical reduction method can be also used as a way to synthesize Cu nanoparticles with different sizes by using the CuO nanoparticles of different sizes as the electrode.

Conclusion

Well-dispersed cupric oxide (CuO) nanoparticles with the size from 10 to 100 nm were successfully synthesized by thermal decomposition of CuC_2O_4 precursor at 400 °C. The electrochemical tests showed an interesting phenomenon that the larger average size of the particles is, the smaller discharge capacity of the first time is, while that of the second time is larger. We have also synthesized the copper nanoparticles with different sizes by using the cupric oxide with different sizes as the electrodes. And this method can be realized easily and controlled elegantly via the discharge process of CuO/Li cells. We think that other metal oxide powders may also be electrochemically synthesized in the reduction reactions, indicating a new synthesis method to fabricate nanosized metals.

Fig. 6 FESEM images of the Cu particles by treated with (**a**) electrode a, (**b**) electrode c
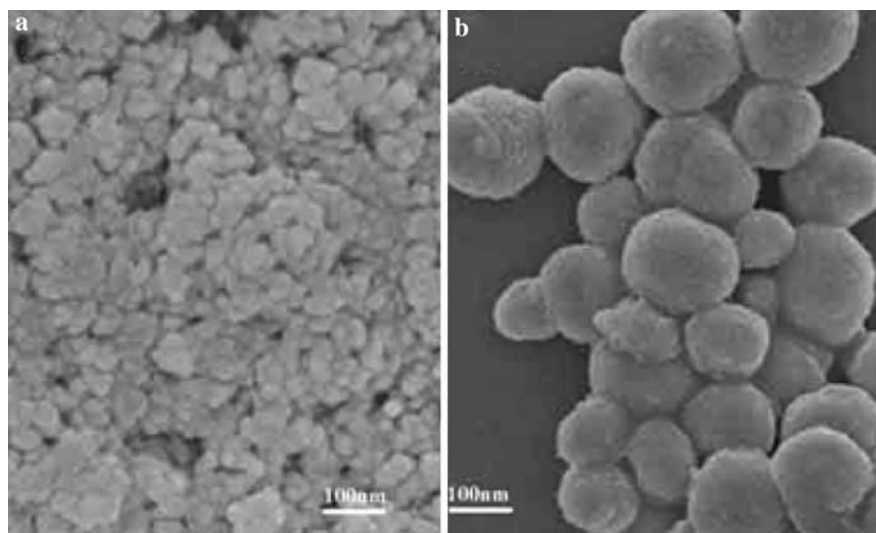
References

Chang SK, Kim HJ, Hong ST (2003) Alternative anode materials for lithium-ion batteries: a study of Ag$_3$Sb. J Power Sources 119:64–68

Debart A, Dupont L, Poizot P, Leriche JB, Tarascon JM (2001) A transmission electron microscopy study of the reactivity mechanism of tailor-made CuO particles toward lithium. J Electrochem Soc 148(11):1266–1274

Gao XP, Bao JL, Pan GL, Zhu HY, Huang PX, Wu F, Song DY (2004) The preparation and electrochemical performance of polycrystalline and single crystalline CuO nanorods as anode materials for Li ion battery. J Phys Chem B 108:5547–5551

Grugeon S, Laruelle S, Urbina RH, Dupont L, Poizot P, Tarascon JM (2001) Particle size effects on the electrochemical performance of copper oxides toward lithium. J Electrochem Soc 148:285–292

Ha HW, Joeng KH, Kim K (2006) Effect of titanium substitution in layered LiNiO$_2$ cathode material prepared by molten-salt synthesis. J Power Sources 161:606–611

Kalaiselvi N, Raajaraajan AV, Sivagaminathan B, Renganathan NG, Muniyandi N, Ragavan M (2003) Synthesis of optimized LiNiO$_2$ for lithium ion batteries. Ionics 9:382–387

Kim TJ, Son D, Cho J, Park B (2006) Enhancement of the electrochemical properties of β-LiMnO$_2$ cathodes at elevated temperature by lithium and fluorine additions. J Power Sources 154:268–272

Liu HS, Yang Y, Zhang JJ (2006) Investigation and improvement on the storage property of LiNi$_{0.8}$Co$_{0.2}$O$_2$ as a cathode material for lithium-ion batteries. J Power Sources 162:644–650

Ng SH, Wang JZ, Wexler D, Konstantinov K, Guo ZP, Liu HK (2006) Highly reversible Lithium storage in spheroidal carbon-coated silicon nanocomposites as anodes for lithium-ion batteries. Angew Chem Int Ed 45(41):6896–6899

Novak P (1985) CuO cathode in lithium cells-II. Reduction mechanism of CuO Electrochim. Acta 30:1687–1692

Novak P, Klapste B, Podhajecky P (1985) CuO cathode in lithium cells: I. influence of the decomposition conditions of Cu(OH)$_2$ on the properties of CuO. J Power Sources 15:101–108

Ozawa K (1994) Lithium-ion rechargeable batteries with LiCoO$_2$ and carbon electrodes: the LiCoO$_2$/C system. Solid State Ionics 69:212–221

Park MS, Yoon WY (2003) Characteristics of a Li/MnO$_2$ battery using a lithium powder anode at high-rate discharge. J Power Sources 114:237–243

Podhajecky P (1985) The influence of preparation conditions on the electrochemical behaviour of CuO in a Li/CuO cell. J Power Sources 14:269–275

Podhajecky P, Scrosati B (1985) Copper oxide cathodes for lithium organic electrolyte batteries. J Power Sources 16:309–317

Poizot P, Laruelle S, Grugeon S, Dupont L, Tarascon JM (2000) Nano-sized transition-metaloxides as negative-electrode materials for lithium-ion batteries. Nature 407:496–499

Ritchie A, Howard W (2006) Recent developments and likely advances in lithium-ion batteries. J Power Sources 162:809–812

Scrosati B (1995) Challenge of portable power. Nature 373(16):557–558

Shembel E, Apostolova R, Nagirny V, Kirsanova I, Grebenkin Ph, Lytvyn P (2005) Electrolytic molybdenum oxides in lithium batteries. J Solid State Electrochem 9:96–105

Tarascon JM, Armand M (2001) Issues and challenges facing rechargeable lithium batteries. Nature 414:359–367

Wang ZX, Chen LQ (2005) Solvent storage-induced structural degradation of LiCoO$_2$ for lithium ion batteries. J Power Sources 146:254–258

Wang X, Song JM, Gao LS, Jin JY, Zheng HG, Zhang ZD (2005) Optical and electrochemical properties of nano-sized NiO via thermal decomposition of nickel oxalate nanofibres. Nanotechnology 16:37–39

Yuan L, Guo ZP, Konstantinov K, Liu HK, Dou SX (2006) Nano-structured spherical porous SnO$_2$ anodes for lithium-ion batteries. J Power Sources 159:345–348

Zhang J, Xie S, Wei X, Xiang YJ, Chen CH (2004) Lithium insertion in naturally surface-oxidized copper. J Power Sources 137:88–92

Zhang DW, Yi TH, Chen CH (2005) Cu nanoparticles. derived from CuO electrodes in lithium cells. Nanotechnology 16:2338–2341

Zhang SS, Xu K, Jow TR (2006) Study of the charging process of a LiCoO$_2$-based Li-ion battery. J Power Sources 160:1349–1354

Zhou F, Zhao XM, Zheng HG, Shen T, Tang CM (2005a) Low-Temperature Refluxing Synthesis of Nanosized LiMn$_2$O$_4$ Cathode Materials. Chem Lett 34:1270–1271

Zhou F, Zhao XM, Zheng HG, Shen T, Tang CM (2005b) Synthesis and electrochemical properties of ZnO 3D nanostructures. Chem Lett 34:1114–1115